Northumbria Research Link

Northumbria
University
NEWCASTLE

Experimental Investigation of CFRP-Strengthened Steel Beams with Web Openings

Mohammed J. Altaee[1,2], Lee S. Cunningham[1], Martin Gillie[3]
[1]University of Manchester, School of Mechanical, Aerospace & Civil Engineering, Manchester, UK
[2]University of Babylon, College of Engineering, Hilla, Iraq.
[3]University of Warwick, School of Engineering, Coventry, UK

Abstract

The introduction of web openings in existing steel floor beams is a common occurrence in practice. Such modifications are often necessary to accommodate additional services driven by a change of building use, thus extending the service life of the structure. Depending on their size and location, openings in the web can present a major challenge to the strength and stiffness of the beam. Strengthening around an opening is often necessary to maintain the required performance of the floor beam, traditionally this is affected via application of additional steel plate, either bolted or welded. This paper focusses on the novel application of carbon fibre reinforced polymer (CFRP) to the problem of strengthening web openings, taking advantage of the material's ease of handling, superior strength-to-weight ratio and corrosion resistance. An experimental study involving 4 full scale universal beams was conducted in order to investigate the ability of CFRP to recover the strength and stiffness of beams following the introduction of web openings. All the specimens were tested under 6-point bending in the experiments. For further comparison, the equivalent test series without the addition of strengthening was modelled numerically via finite element analysis.. The effectiveness of the strengthening technique was demonstrated with increases in the load carrying capacity over the un-altered beam of between 5 and 20% being achieved.

Keywords: CFRP, retro-fitting, steelwork, strengthening, web-openings

1. Introduction

Alteration and adaption of existing buildings often involves introduction of web openings in steel beams to accommodate additional services. This process clearly has a detrimental effect on the beam's load capacity and is conventionally mitigated via welding of additional steel pate as outlined in SCI355 [1]. Although popular, this method has the drawback of in-situ welding and the associated practical and health and safety implications. An alternative to this method of strengthening is to use fibre reinforced polymer composite plate bonded to the surface of the steel. Carbon fibre reinforced polymers (CFRP) have been used increasingly in structural strengthening instead of steel plates in the last 20 years or so, albeit outside the context of steelwork with web openings. CFRP has significant advantages over steel, in particular a superior strength to weight ratio and excellent resistance to corrosion.

A signifiant number of experimental, numerical and theoretical studies have been undertaken on externally bonded CFRP with steel members, examining various parameters in order to investigate the advantages of this strengthening method. Several studies applied CFRP to the bottom flanges of steel sections as a repair or strengthening means. Deng & Lee [2] used different lengths and thicknesses of CFRP (E=212GPa) in strengthening ten 127×76×13UKB steel I-sections of 1100 mm span under either three or four point static bending. It was concluded that the de-bonding mode of failure was initiated at lower load levels when the CFRP plate thickness increased and its length decreased. The maximum gain in strength (30%) was achieved in the beam with the longest bonded length (500 mm) and thinnest CFRP plate thickness (3 mm). Colombi & Poggi [3] tested four steel beams (HEA 140, 133×140×25.1, European wide flange beams) of 2500 mm span under static three-point bending. The beams were strengthened with two 120×1.4 mm layers of CFRP plate (E=200GPa) and the ends of the CFRP plates were wrapped with CFRP sheets which were extended up along the web to provide anchorage and prevent debonding. Although the tests were terminated before failure after excessive deflections were observed at mid-span, the results showed that the stiffness and load capacity achieved an increase of 14% and 40%, respectively over the un-strengthened section.

Patnaik & Bauer [4] used four fabricated I-section beams without openings. Two beams (324×152.5mm) were reinforced by CFRP strips along the tension flange and exposed to a flexural failure test. Four point bend tests

were performed in all those tests. The other two beams (355.5×254mm) were reinforced by CFRP strips along their webs and exposed to a shear failure test. The first two recorded a 14% increase in the flexural capacity. For the two shear-strengthened beams, one failed locally at the weld returning a 15% load enhancement while the other recorded a 26% increase in strength.

The majority of strengthening studies report that debonding at the ends of the CFRP is the governing failure mode for this kind of strengthening due to the associated peak shear stresses. Investigations by both Deng & Lee [2] and Linghoff et al. [5] found the maximum stress in the CFRP occurred approximately 20mm from the ends of the strengthening at the mid-span. In order to study the influence of CFRP laminate geometry on end de-bonding, Rizkallaa et al. [6] examined the effect of tapering the adhesive in section and on-plan at the ends of the CFRP plate. It was found that strain reduced by 59% at the ends of the CFRP with on-plan tappers and tapering in section at the ends compared with square and flush finished ends. This suggests the beam load capacity could be increased with this process due to delay of CFRP debonding.

Narmashiri et al. [7] studied the effect of using mechanical fixing clamps to avoid debonding. Clamps were formed by bolting the CFRP to the steel. The beams were tested under four point loads. The results show that the load capacity increased by 24% compared to that of the non-clamped, adhesive-fixed plate.

Some research has been conducted on damaged steel beams to simulate the effect of corrosion. Liu et al. [8] tested artificially notched steel beams under three-point bending tests. The beams were W12×14 US steel sections (length = 2438 mm) with a 106 mm notch in the tension flange. CFRP laminates of 100 mm width were used to cover the notch with different lengths at the tension flange: along the entire length, and along a quarter of the beam length. Use of CFRP caused an increase of 60% and 45% in the load capacity for the full length and quarter length specimens respectively. Tavakkolizadeh & Saadatmanesh [9] used four-point bending on two groups of S5×10 US steel I-section beams (length = 1300 mm) which were notched in the middle of the tension flange to depths of 3.2 mm for the first group and 6.4 mm for the second group. Both groups were reinforced by different lengths of CFRP sheets with 0.13 mm thickness. The results showed that the ultimate load carrying capacity and stiffness of the retrofitted specimens were close to their original values in the control specimen regardless of the length of the CFRP patch. The results of the deep notched group showed distinct loss of ductility in comparison with the shallow group.

The existing research on strengthening is not confined to carbon fibre reinforced polymer, Okeil et al. [10] applied glass fibre reinforced polymer (GFRP) strengthening at the end web panels of ASTM A36 steel plate-girders (533.4×280) to strengthen against web buckling, the girders were tested under three point loading. The test results showed that the ultimate load capacity of specimens with vertical and diagonally placed GFRP stiffeners could be increased by 40% and 56% respectively.

Despite these varied studies, to date there is no readily available experimental study on the behaviour of CFRP strengthened steel beams with web openings. Altaee et al.[11],[12] investigated numerically the behaviour of CFRP strengthened steel beams with openings subjected to uniformly distributed quasi static loads and different strengthening arrangements. In the numerical study, it was found that CFRP plates can recover beam strength and stiffness after web opening introduction. It was also found that there is an optimum arrangement of CFRP both in terms of thickness, length and location, beyond which the strength enhancement is negligible due to debonding effects. Several strengthening configurations were investigated with the most effective being application of CFRP around the opening to the top flange (underside), bottom flange (underside) and web as shown in Figure 1.

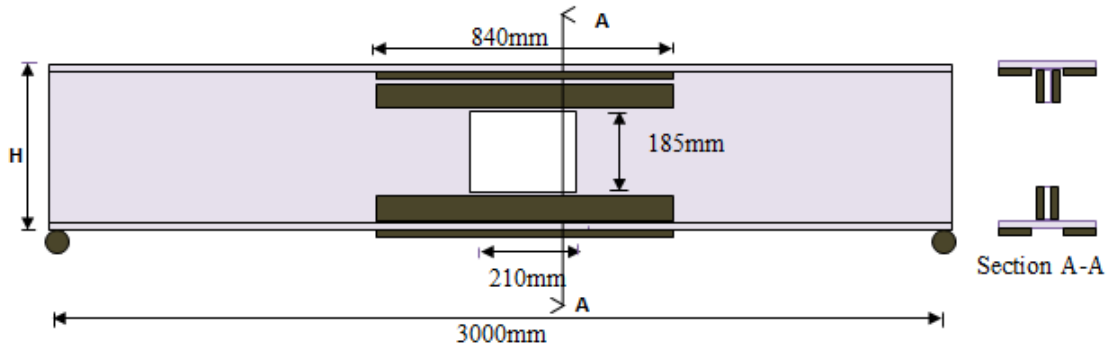

(a) B1-RO

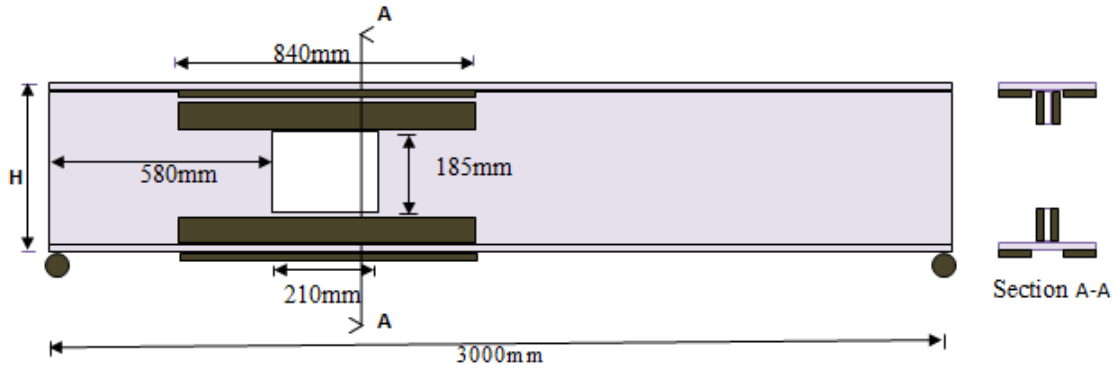

(b) B2-RO

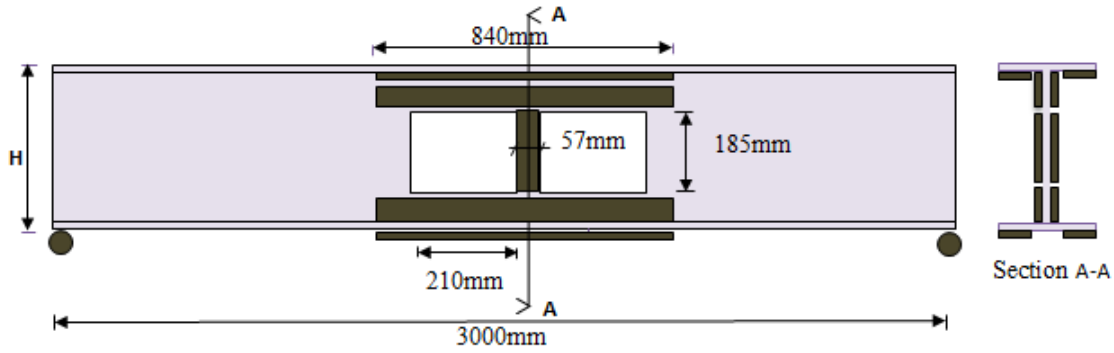

(c) B3-RO

Figure 1 Layout of strengthened specimens and boundary conditions.

For the specific case of beams with web openings, a number of different failure modes are possible depending on the position and size of the opening as shown in Table 1.

Table 1 Failure modes of steel beams with openings [11],[12].

Due to the position of the opening in the maximum moment and low shear region (mid- span of a simply supported beam), yield may occur in the tee-sections above and below the web openings, this may be initiated or followed by lateral buckling of the tee (depending on level of restraint).	 Flexural Failure
A Vierendeel type failure is associated with high shear forces acting on the beam in the region of a web-opening. As a result, four plastic hinges are formed at the corners of the web opening.	 Vierendeel or Shear Failure
Web-post buckling failure is associated with high compression forces acting on the top flange above the opening which results in excessive bending of the tee-section. This may in turn initiate buckling in the top tee itself and/or flexural buckling of the web-post.	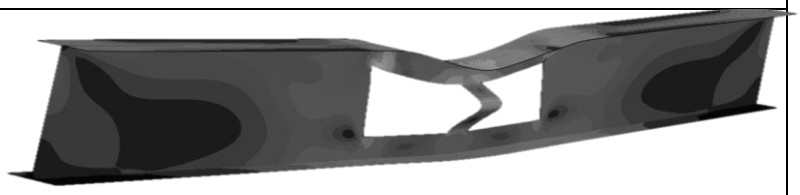 Web-Post Buckling

The focus of this paper is to investigate experimentally the capability of CFRP plates to recover the strength and stiffness of steel I-beams after the introduction of web openings under static loading using the configurations previously investigated numerically by Altaee et al.[11],[12]. Using a purpose-built test rig, four samples were tested with different web-opening positions aimed at examining the different failure modes.

2. Experimental Setup

2.1 Specimen Description

The experimental series consisted of 4 no. 305×102×25 UKBs with 3m clear span; one without an opening acting as the control (B0), and three with rectangular web openings in different locations (B1-RO, B2-RO & B3-RO, where RO denotes “Reinforced/strengthened Opening”) as shown in Figure 1.

2.2 Loading & Boundary Conditions

The typical uniform load delivered by a floor slab in practice was represented using a rigid steel frame comprising three UC beams. All the specimens were tested under 6-point bending to approximate a uniformly distributed load as shown in Figure 2.

Triangulated steel frames were fabricated from I-sections (178×102×28 UKB) to form lateral restraints, these were distributed along the beam length at 900mm c/c as shown in Figure 2. In order to allow the specimen to deflect vertically and minimise friction effects between the lateral support and the specimen, rigid steel spacers in combination with 10mm thick PTFE plates were adopted. The steel roller supports at each end of the beam were used to provide horizontal translations shown in Figure 3.In addition, 130mm wide bearing plates at the supports were added to prevent premature web bearing and buckling failure, in accordance with Eurocode 3[13].

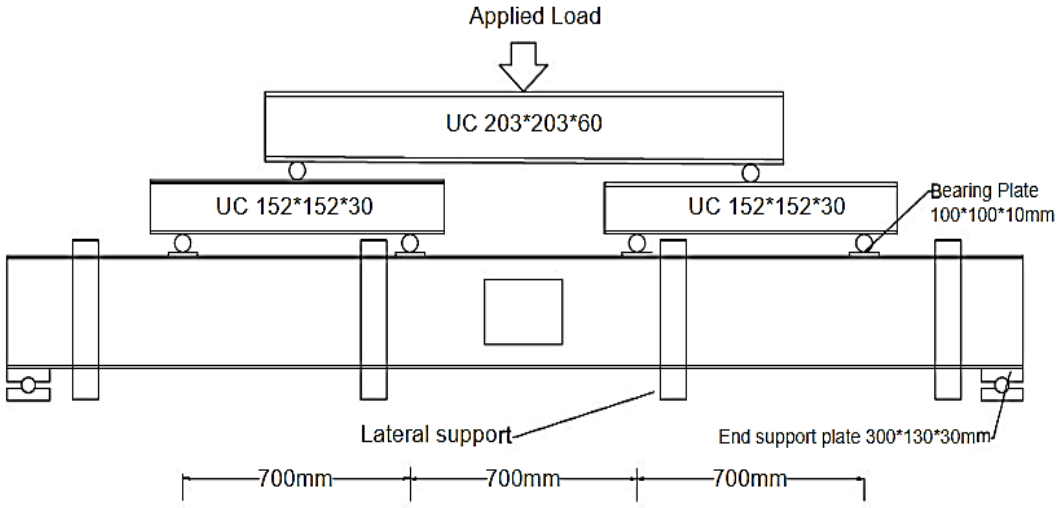

(a) Elevation

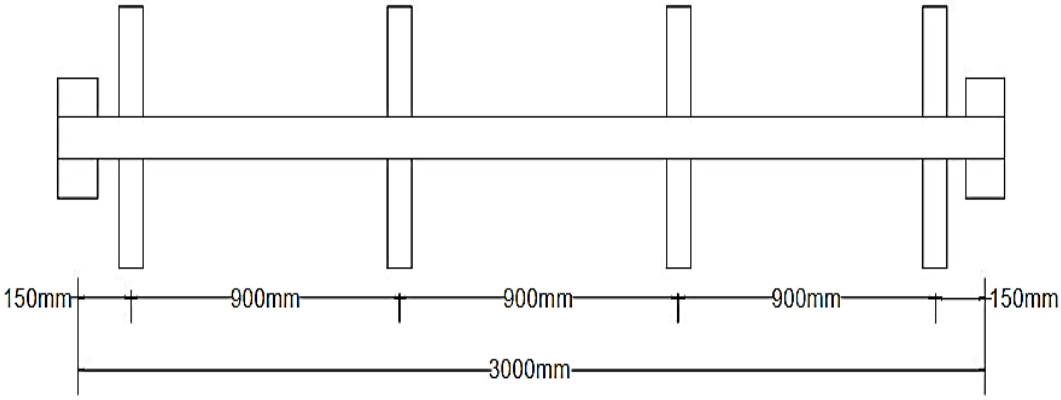

(b) Plan view

(c) General layout

Figure 2 Test load configuration.

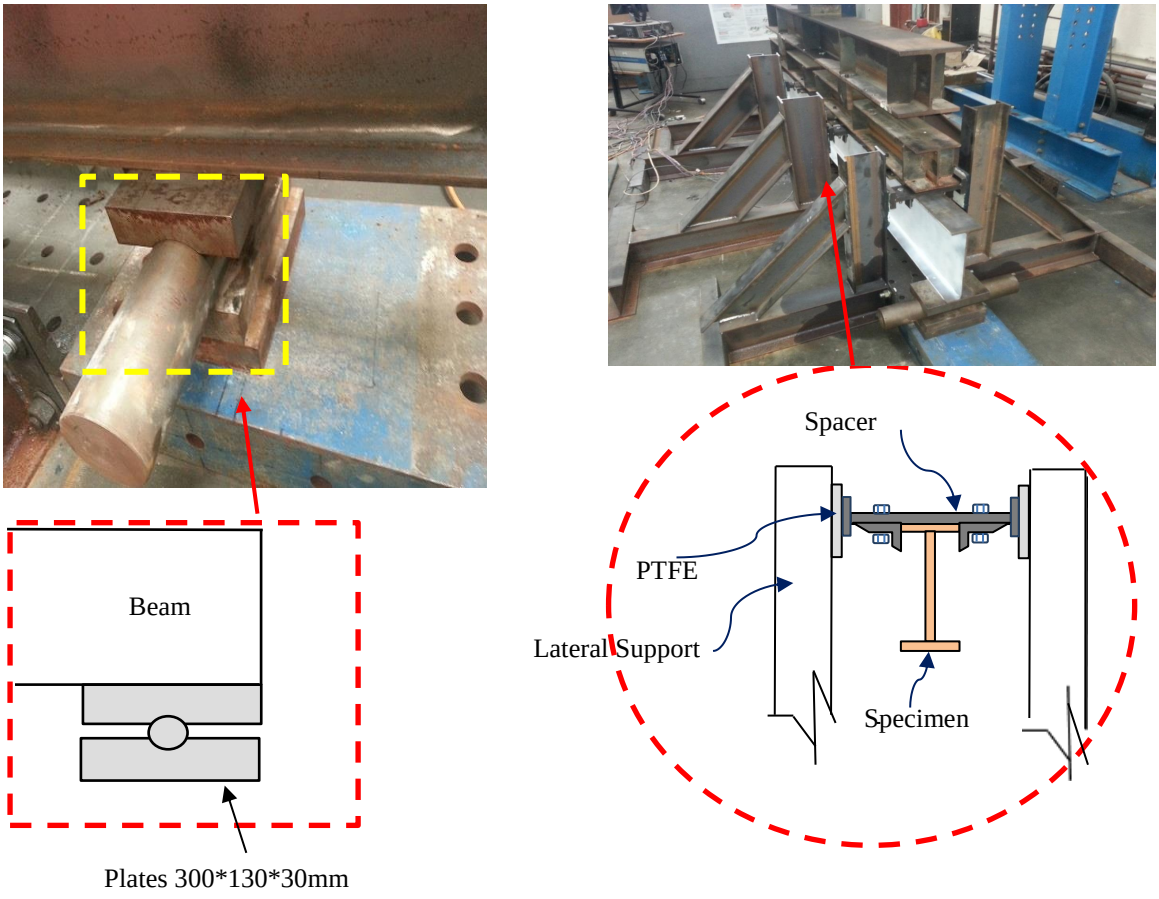

(a)End support (b) Lateral support

Figure 3 End support and lateral support description.

2.3 Specimen preparation

Each specimen had a 3000mm clear span. One or two 230 x 185mm web openings were formed in different places over the specimen length using an electric cuter. Prior to cutting, 5mm holes were formed at the opening corners to avoid notch formation.

In order to achieve the best bond between steel and CFRP, mechanical grinding was employed to remove the weak oxide layer. Then, the ground surface was cleaned with acetone to remove any grease or oil before applying the epoxy and CFRP layer.

2.4 Specimen Material Properties

To determine the mechanical strength of the steel used in the I-sections of the test series, tensile coupon tests were carried out to the specifications and guidelines in BS EN 10002-1[14]. Three coupons were taken from two un-yielded locations (one flange and one web) of the four steel beams tested. The average yield and the average ultimate stresses for flange and web were determined by averaging the results obtained from all the tensile coupon tests as shown Table 2. The average stress-strain curve for each series is shown in Figure 4. Unidirectional CFRP plates, 3mm thick, were provided by Weber [15]. The CFRP modulus of elasticity was 200 GPa, and the tensile strength was 2400MPa, based on the manufacturer's details. The CFRP plates were manufactured using a pultrusion process and had a fibre volumetric content of 70% in an epoxy resin matrix. Two components of epoxy were used to bond the CFRP plates to the specimens. The epoxy (Araldite 420) is manufactured by Araldite Co. [16] with properties as shown in Table 3.

Table 2 Summary of the mechanical properties of steel (mean values shown).

	Young's Modulus (GPa)	Yield stress(MPa)	Ultimate tensile stress(MPa)
Flange	206	412	566
Web	210	435	569

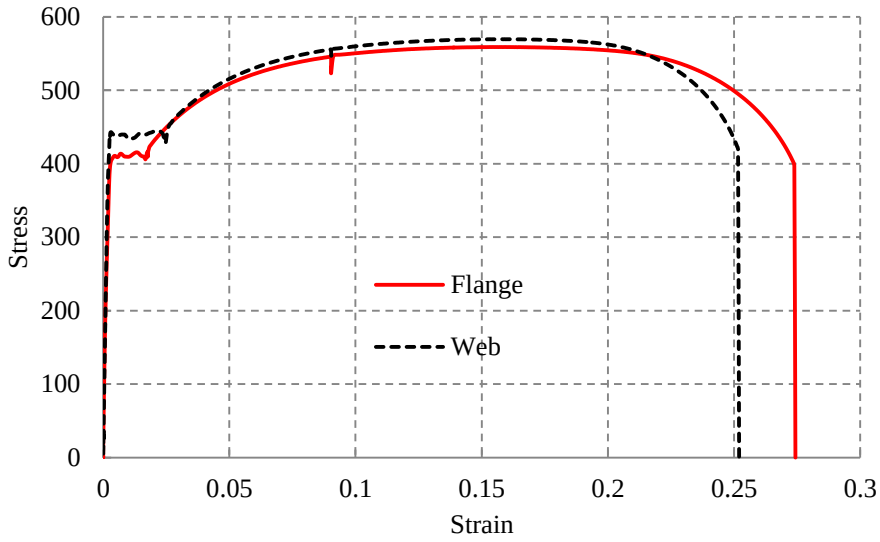

Figure 4 Mean tensile stress-strain relationship from coupon tests.

Table 3 Summary of the mechanical properties of Araldite 420 epoxy adhesive when cured at room temperature for 24 hours [16].

Young's Modulus (GPa)	Ultimate Tensile strength (MPa)	Ultimate Shear strength (MPa)	Strain at rupture %
1.5	29	26	4.6

2.5 Installation of the CFRP plates

The CFRP plates were first cut to the desired length and their edges were ground to obtain a flat, smooth surface. Then the resin/hardener components of the epoxy were mixed together with ratio of 1:2.5 by weight [16]. 1mm glass beads were used in the mix at a 1% dosage to achieve a constant thickness for the epoxy layer.

After cleaning the CFRP plates from dust, the adhesive was applied in a triangular form to allow even dispersal and then the plate was placed immediately on the designated location. Next, when the CFRP was placed on the

steel beam, the adhesive was squeezed out from the centre to the sides, thereby reducing the possibility of air pockets in the adhesive layer. The composite was left to cure before bonding the other face of the specimen

In order to prevent any sliding or shifting in the CFRP plate positions, a 10mm steel plate was placed over the CFRP with a PTFE separation layer to avoid unintentional bonding as shown in Figure 5.

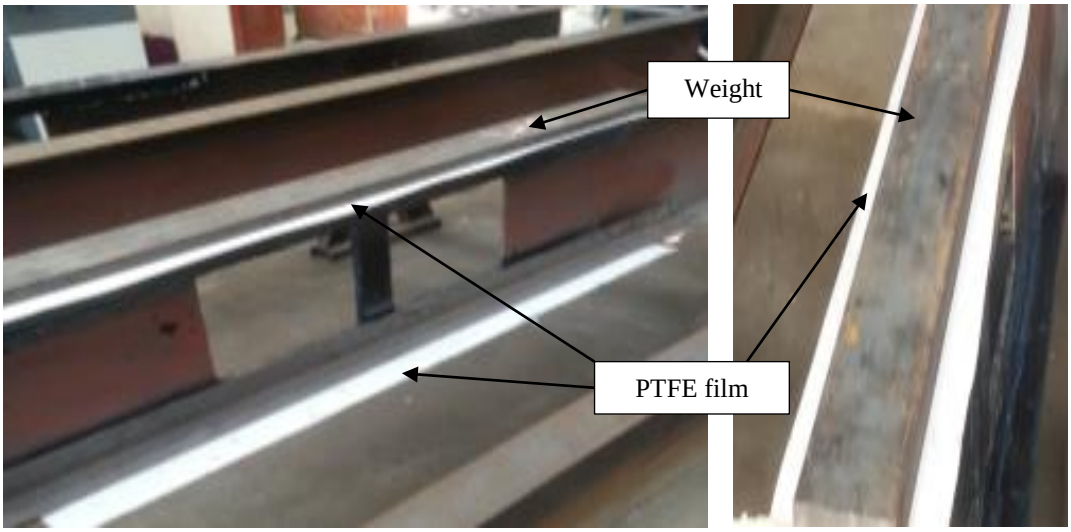

(a) Fixing of CFRP plates showing temporary weight during curing

(b) Upturned specimens during curing of adhesive

Figure 5 CFRP plate application process.

2.6 Strain and deflection measurement

Strain gauges were mounted on every CFRP strip parallel to the fibre direction, and on each specimen at 20mm from the plate end in view of the findings of Deng et al. [17] and Linghoff et al. [5] in which they recorded maximum shear stresses in this location, details are shown in Figure 6. Linear Variable Displacement Transducers (LVDT) were positioned underneath the specimens at mid-span to measure the vertical displacement during the test. Moreover, rosette strain gauges were mounted on the steel web near the opening corner to measure the steel strain in three directions X, Y and XY.

All beams were tested under displacement control with a rate of 2mm/min using a 500 kN capacity INSTRON Universal Testing Machine. Loads and dial gauge readings were recorded at each of these increments.

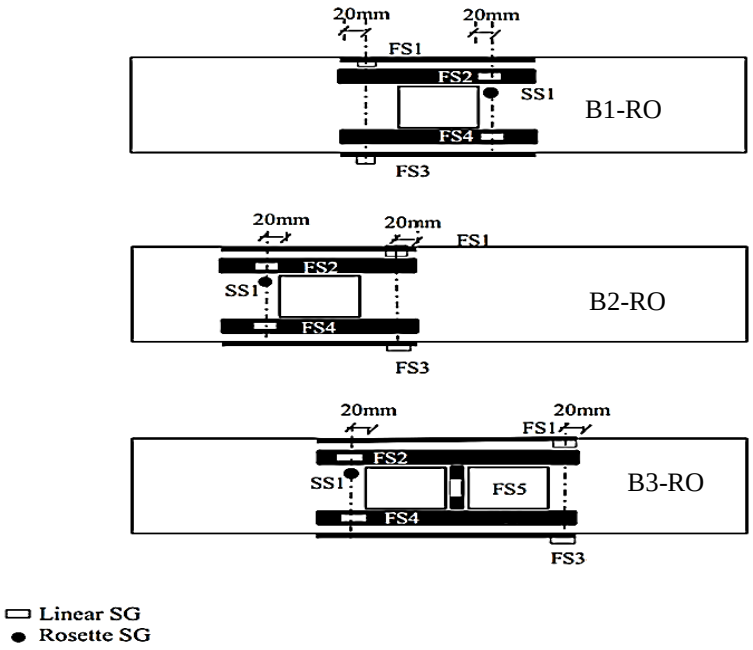

Figure 6 Strain gauge layout, specimens B1-RO to B3-RO.

3. Results and Discussion

The following section describes the results from the test series. For economy, only the strengthened beams with openings were tested experimentally. In order to compare the performance, the un-strengthened versions of B1-RO, B2-RO & B3-RO (denoted B1-UO, B2-UO & B3-UO respectively, where UO stands for "Un-strengthened Opening") were modelled using non-linear finite element analysis via Abaqus [18]. The model was validated in previous studies by the authors, Altaee et al. [11][12]. The experimental behaviour of the control beam B0 provided further opportunity to validate the model for the unstrengthened beams. The general purpose 4-node shell element S4R with reduced integration was adopted for the steel section. The mesh comprised of 15mm x 15mm sized elements (based on a previous mesh sensitivity study, [12]). Geometric nonlinearity and material nonlinearity were included in the analysis. For each beam, an initial geometric imperfection of span/1000 based on BS EN 1090-2 [19] was adopted in the analysis. The Abaqus/Explicit solution procedure was adopted since this has been shown to be suitable for quasi-static loading situations involving high non-linearity [18].

3.1 Un-strengthened Beams B0, B1-UO, B2-UO & B3-UO

The numerical load displacement relationship for B1-UO to B3-UO together with the experimental model and numerical result for the control beam B0 (denoted as B0-Exp and B0-FE respectively) is presented in Figure 7.

For benchmarking purposes, the Eurocode 3 [13] derived design strength of B0 has been included in Figure 7. According to Eurocode 3, for a yield strength of 412 N/mm^2, and effective length of 900mm, the moment capacity of B0 should be 130kNm with failure governed by lateral-torsional buckling (the fully restrained i.e. zero effective length moment capacity = 140 kNm), which corresponds to an ultimate total load of around 322kN for the 6-point bending configuration examined. At the early stages of the experiment on B0, a linear elastic response was observed upto around 300 kN. Beyond this point, the onset of localised yield in the top flange at mid-span was observed. Concurrent with this, visible rotation of the top flange at mid-span was noted. On further loading, lateral torsional buckling in the constant moment zone between the central lateral restaints was observed as the beam eventually reached a peak load of 406kN. At this point a full plastic hinge was developed at the mid-span top flange (see Figure 8a). The experimental unloading branch of the beam was captured following dipslacement control procedure until the rotation of the top flange reached a point at which the test was stopped. The numerical model shows good agreement with the experimental results (Figure 7), with occurrence of yield in the top flange and onset of lateral torsional buckling between the mid-span restraints at around 350kN.

As would be presumed, the FE results show that beams B1-UO, B2-UO & B3-UO all failed at lower load levels than B0, around 15% on average and in the case of B2-UO a noticeably less stiff repsonse was observed. With its central opening, B1-UO represents a 15% reduction in the plastic modulus (and associated reduction in local moment capacity) compared to B0. In the case of beam B1-UO, after linear load behaviour up to around 350kN, significant torsional rotation started in the top T-section above the central opening, this also corresponded with the development of a plastic hinge in the top T-section at mid-span. After peaking at around 357kN, unloading of the beam was accompanied by further lateral buckling of the section between the central restaints, see Figure 9. For beam B2-UO, yielding occured in both corners around the opening at a load of around 330kN, consistent with the Vierendeel action described in Table 1. In beam B3-UO, yielding was observed in the top flange around both openings after yielding in the central portion, web-post buckling was initiated at a load of around 350kN.

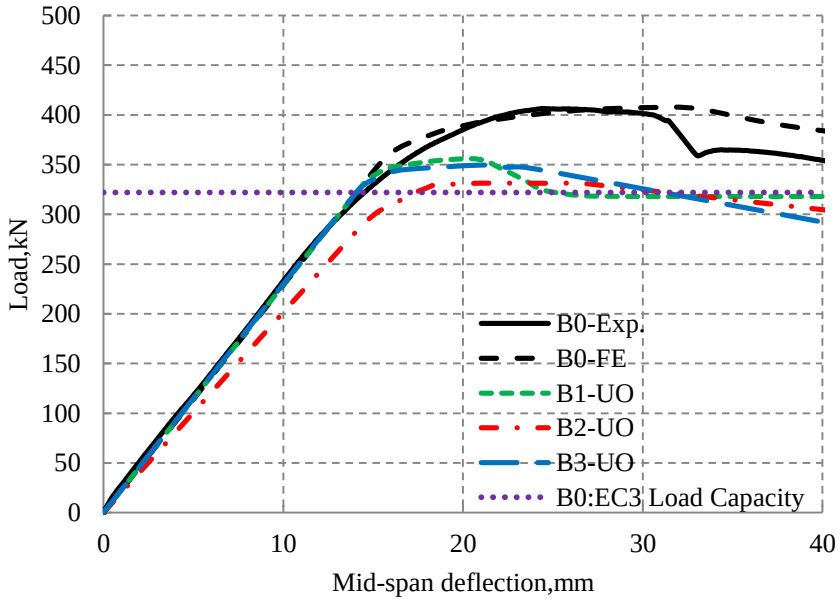

Figure 7 Load versus vertical displacement at mid-span: specimens B0 & B1-UO to B3-UO.

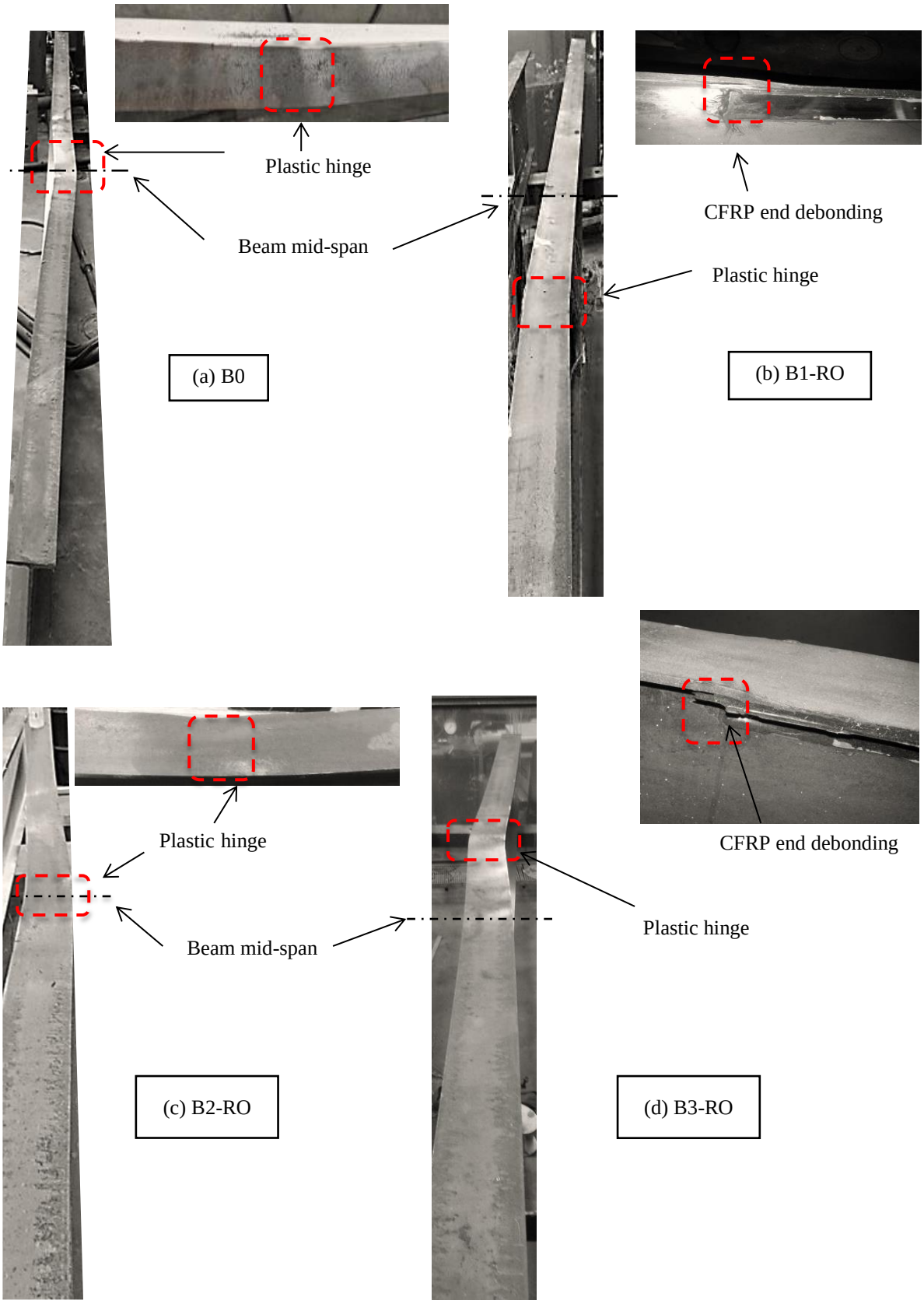

Figure 8 Failure patterns for Specimens B0 & B1-RO to B3-RO.

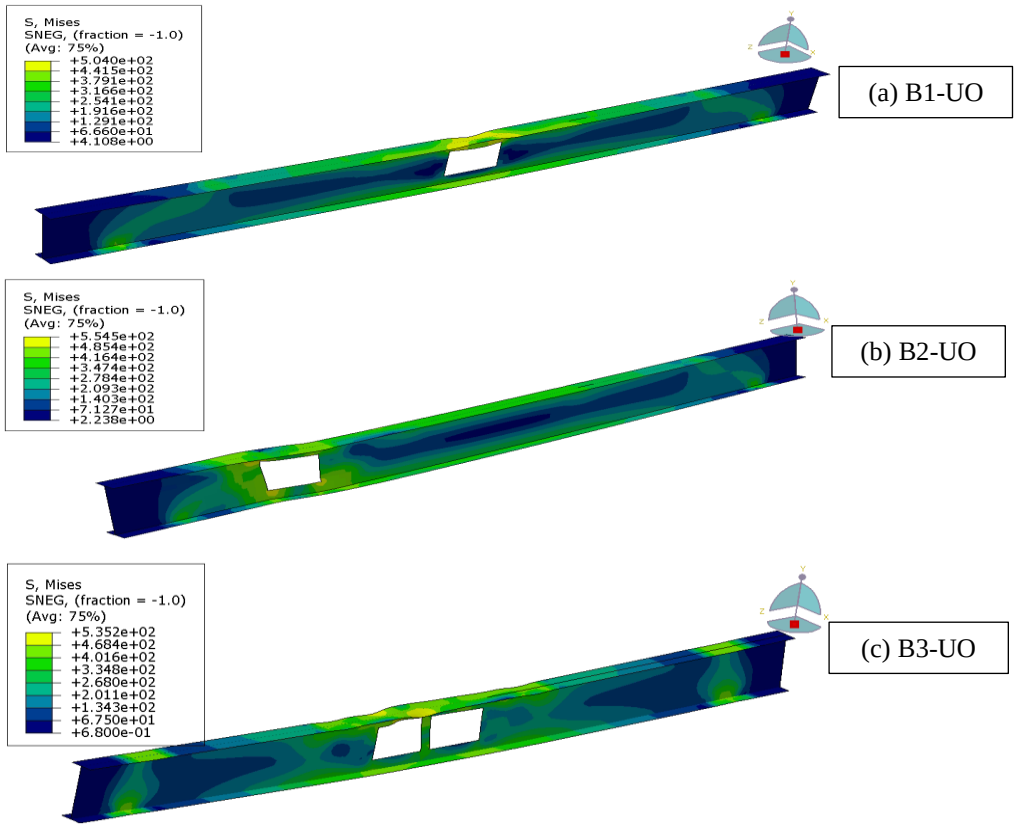

Figure 9 Von Mises stress distribution (N/mm^2) and deflected shape at ultimate load.

3.2 Strengthened Beams B1-RO, B2-RO & B3-RO

Figure 10 compares the experimental load-displacement response of strengthened beams B1-RO to B3-RO with the unstrengthened control beam B0. In all strengthened cases a stiffer response is obtained accompanied by an increase in peak load. A summary of the results is given in Table 4.

Specimen B1-RO

Due to the presence of the CFRP plates, the stiffness of B1-RO was significantly increased in comparison with un-strengthened specimen B0. B1-RO exhibited a fairly linear trend up to a load of approximately 435 kN. Beyond this load level, there was evidence of the onset of plastic hinge formation in the top flange near the end of the CFRP plate. This is corroborated by the strain gauge output from FS1 (Figure 11a), which suggests onset of steel yielding (2000 microstrain), assuming strain compatibility between the CFRP and the steel. Lateral torsional buckling of the section between the central lateral restraints was observed to start at around 470 kN. At this point, debonding of the CFRP commenced in the top flange at the extreme edge away from the opening. Strain gauges FS2, 3 and 4 all recorded comparatively low strains indicating the CFRP strengthening in these locations was not working hard. The test was continued until a load level of 488kN, beyond this point the test was stopped due to excessive lateral deflection. The final deflected shape of the beam, including the plastic hinge location is shown in Figure 8b.The strain rosette readings from SS1 indicate that yielding did not take place in the web, Figure 12a.

Specimen B2-RO

In comparison to B1-RO, a less-stiff response was obtained. Lateral torsional buckling commenced at around 405kN in the zone between the central lateral restraints. Onset of yielding was recorded at the opening corners before reaching the ultimate load, see FS4 and SS1-XY in Figure 11b and Figure 12b respectively. As in the case of B1-RO, the test was stopped due to excessive lateral displacement of the top flange and an accompanying drop in load at around 424 kN. The final deformed shape of the beam is shown in Figure 8c. The failure mode of B2-RO was different than in the numerical model of the corresponding unstrengthened beam B2-UO. In B2-RO plastic hinge formation at the mid-span top flange and lateral torsional buckling controlled,

while Vierendeel action and associated yielding around the corner opening dominated the behavior of B2-UO. This change in failure pattern demonstrates the influence of the CFRP strengthening on the stress state of the member. Observation of Figure 7 shows that B2-UO achieved an ultimate load 334 kN (compared to 405.8 kN for B0). Use of the CFRP strengthening arrangement allowed B2-RO to recover and surpass the full strength of B0 resulting in a 5% strength enhancement. Although FS4 indicated the strain in the CFRP at this location was relatively high, no debonding occurred in the test.

Specimen B3-RO

B3- RO exhibited the same failure mode as B1- RO where lateral torsional buckling of the section between the lateral restraints occurred at around 420kN. Yielding was recorded in the top flange at the CFRP ends before reaching the ultimate load, see FS1 in Figure 11c. In similarity to B1- RO, end debonding of the top flange CFRP commenced at an ultimate load of 442kN. The final deflected shape of the beam, including the plastic hinge location is shown in Figure 8d. The strain rosette readings from SS1 indicate that yielding did not take place in the web at the opening corner, Figure 12c. In contrast to the corresponding un-strengthened beam B3-UO, web post buckling was not observed in the experiment. These observations suggest the CFRP strengthening on the flanges and at the central web post were sufficient to delay onset of this mode, allowing a more global failure mode to develop. Strain gauge FS5 which was mounted at the centre of the web-post strengthening returned modest strains during the test indicating a low utilisation ratio for the CFRP at this location, Figure 11c. Observation of Figure 7 shows that B3- UO achieved an ultimate load of 334 kN (compared to 405.8 kN for B0). Use of the CFRP strengthening arrangement allowed B3- RO to recover and surpass the full strength of B0 resulting in a 10% strength enhancement.

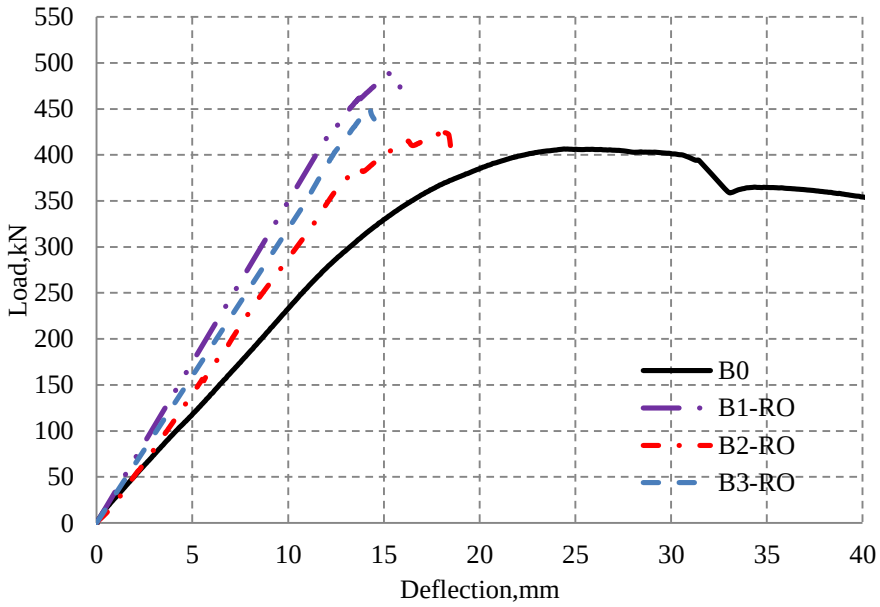

Figure 10 Load versus vertical displacement at mid-span for specimens B0 & B1-RO to B3-RO.

Table 4 Comparison of specimen ultimate load and failure mode.

Specimen	Ultimate load (kN)	Strength difference with B0 (%)	Failure mode* In sequence
B0	405.8	-	LTB+TFY
B1-UO	357	-11.8	LTB+TFY
B2-UO	334	-17.5	YOC+VF
B3-UO	351	-13.3	WPB+TFY
B1-RO	488.3	20	LTB+ TFY +EDC
B2-RO	424	5	LTB+TFY
B3-RO	442	10	LTB+ TFY +EDC

*LTB: Lateral torsional buckling, WPB: Web post buckling, TFY: Top flange yielding,
EDC: End debonding of CFRP, YOC+VF: yielding of opening corner + Vierendeel failure.

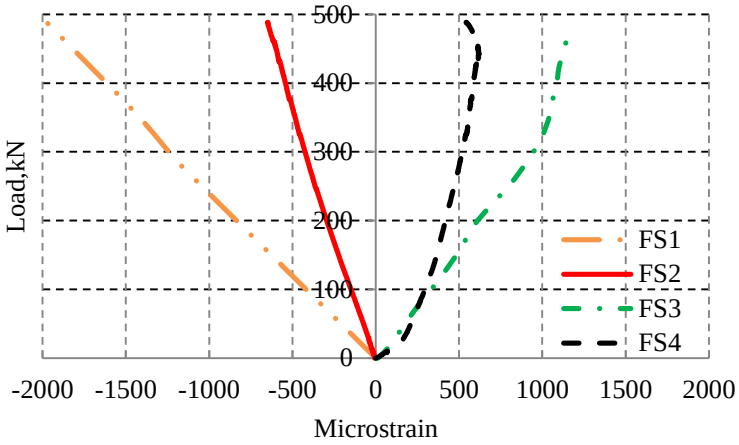

(a) B1-RO

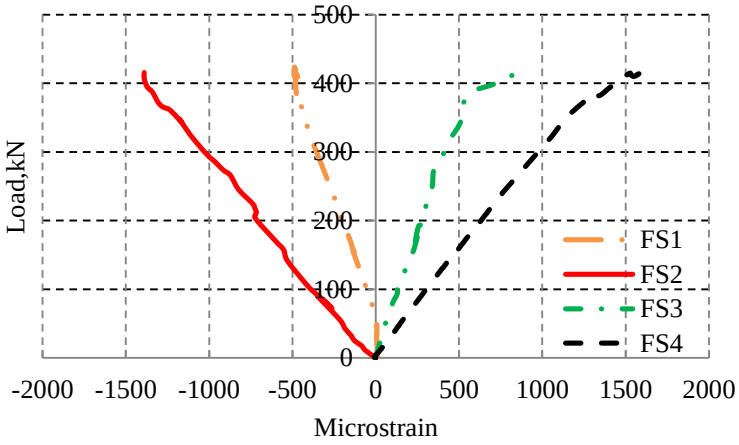

(b) B2-RO

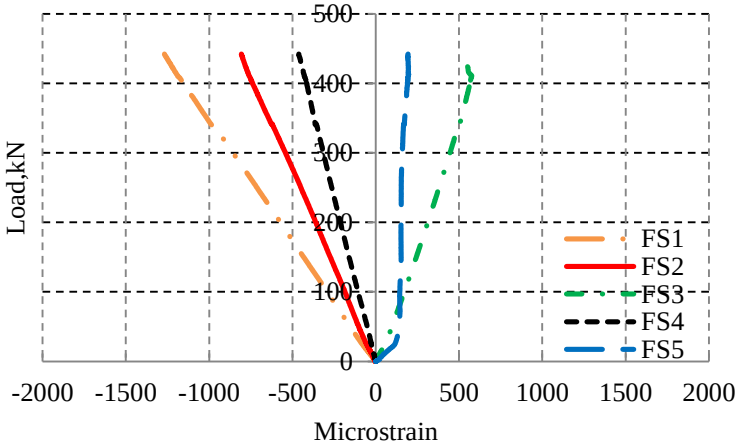

(c) B3-RO

Figure 11 CFRP strain gauge output, B1-RO to B3-RO.

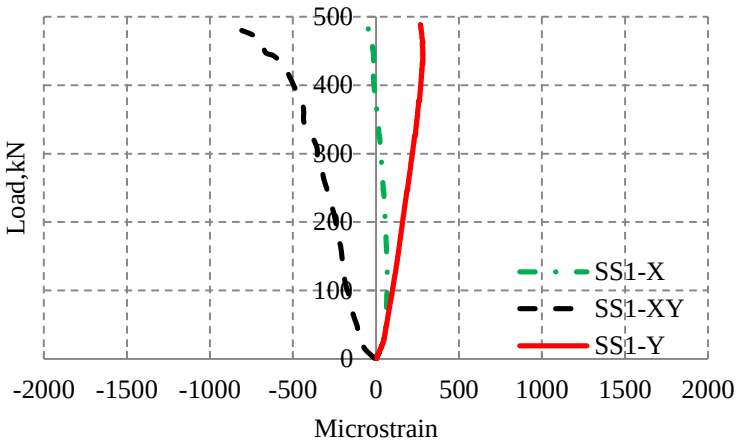

(a) B1-RO

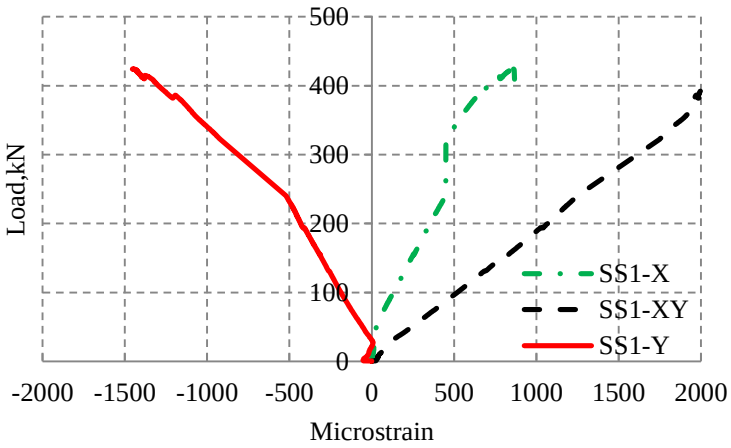

(b) B2-RO

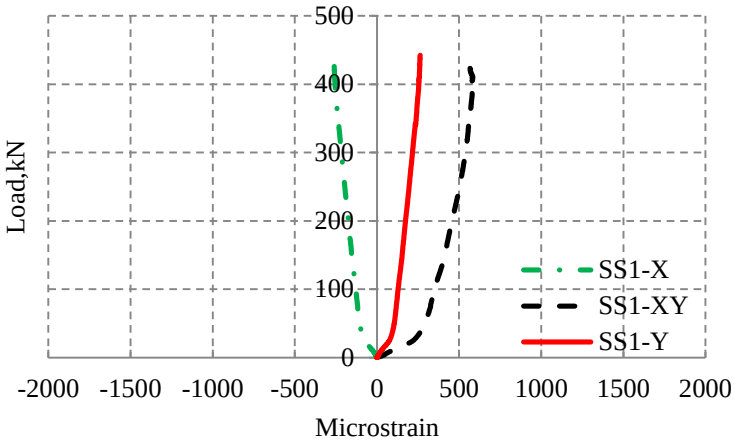

(c) B3-RO

Figure 12 Steel strain gauge output, B1-RO to B3-RO.

4. Conclusions

The purpose of the test programme reported here was to investigate experimentally the ability of CFRP plates to recover the strength of steel beams after the introduction of web openings, and to understand the influence of this strengthening method on the failure modes of such beams. Based on the current study, the most important highlighted points are:

1. For all the strengthened sections examined, a stiffer response was observed up to ultimate load than in the un-strengthened cases. Further, in all cases the strengthened beams showed greater load capacity after strengthening with web openings present than the control case with no openings or strengthening.

2. It is clear that CFRP strengthening can be effective for recovering (and indeed enhancing) both the strength and stiffness of steel beams after the insertion of web openings.

3. The strengthening method is likely to be a useful approach in practice for enhancing both serviceability and ultimate state behaviour of beams where in-service web openings are introduced.

4. The method has benefits over traditional methods such as applying additional steel plate that include lower self-weight, easier application and better corrosion resistance.

5. The failure mechanisms in the strengthened beams were not always the same as in the un-strengthened cases, or the control case. This highlights that if CFRP is used in design, care must be taken to identify and check potential failure mechanisms other than those that might be expected with strengthening.

Although the results have to be viewed within the context of the limited series of tests undertaken, the potential efficacy of the CFRP strengthening approach has been demonstrated. Further work is required to investigate optimisation of the strengthening layouts, with a particular regard to improving the ductility of the strengthened section. In parallel with this, several of the strengthening plates appeared to be under-utilised indicating potential for reduction in plate thickness. Clearly the test series presented is not only limited in terms of the number of specimens, but also in respect of the beam depths and spans examined. Further investigation is required in order to understand possible size effects and define the practical limits of the strengthening approach.

Acknowledgements

The authors gratefully acknowledge the contribution of the Iraqi Ministry of Higher Education and the University of Babylon, Iraq, in funding this research. Thanks are due to Mr Paul Nedwell, Dr Raid Daud and all the laboratory staff at the University of Manchester, School of MACE for their assistance with the experimental program.

References

[1] S. . Hicks and R. M. Lawson, Design of composite beams with large web openings (P355). 2011.

[2] J. Deng and M. M. K. Lee, “Behaviour under static loading of metallic beams reinforced with a bonded CFRP plate,” Compos. Struct., vol. 78, no. 2, pp. 232–242, 2007.

[3] C. Colombi, P. & Poggi, “An experimental, analytical and numerical study of the static behavior of steel beams reinforced by pultruded CFRP strips,” in Composites Part B: Engineering, vol. 37, 2006, pp. 64–73.

[4] A. K. Patnaik and C. L. Bauer, “Strengthening of Steel Beams with Carbon FRP Laminates,” in Proceedings of the 4th Advanced Composites for Bridges and Structures Conference, 2004, p. Calgary, Canada.

[5] D. Linghoff, R. Haghani, and M. Al-Emrani, “Carbon-fibre composites for strengthening steel

structures," Thin Walled Struct., vol. 47, pp. 1048–1058, 2009.

[6] S. Rizkallaa, M. Dawoodi, and D. Schnerch, "Development of a carbon fiber reinforced polymer system for strengthening steel structures," Compos. Part A Appl. Sci. Manuf., vol. 39, no. 2, pp. 388–397, 2008.

[7] K. Narmashiri, N. Ramli Sulong, and M. J. Zamin, "Investigation on end anchoring of CFRP strengthened steel I-beams," Int. J. Phys. Sci., vol. 5, no. 6, pp. 1360–1391, 2010.

[8] X. Liu, P. F. Silva, and a Nanni, "Rehabilitation of Steel Bridge Members with FRP Composite Materials," CCC 2001 Compos. Constr., no. 100 mm, pp. 613–617, 2001.

[9] M. Tavakkolizadeh and H. Saadatmanesh, "Repair of Cracked Steel Girders Using CFRP Sheets," in ISEC-01,Hawaii, 2001.

[10] A. M. Okeil, M. Asce, Y. Bingol, and M. R. Ferdous, "Novel Technique for Inhibiting Buckling of Thin-Walled Steel Structures Using Pultruded Glass FRP Sections," J. Compos. Constr., vol. 13, no. 6, pp. 547–557, 2009.

[11] M. Altaee, L. Cunningham, and M. Gillie, "Novel Technique for Strengthening Steel Beams with Web Penetrations," in Proceedings of the MACE PGR Conference, 2016, pp. 9–11.

[12] M. Altaee, L. Cunningham, and M. Gillie, "CFRP Strengthening of Steel Beams with Web Openings," in Proceedings of Structural Faults & Repair 2016: 16th International Conference, 2016, p. 1754.

[13] BS EN1993-1-1, "Eurocode 3:Design of steel structures," British Standards Institution, London, UK, 2005.

[14] BS EN 10002-1, "Tensile testing of Metallic materials," British Standards Instituion, London, UK, 2001.

[15] Weber Building Solutions, "<http://www.netweber.co.uk/>," ,accessed 10/08/2017. .

[16] Huntsman, "Structural adhesives aerospace adhesives," Araldite 420A/B. Huntsman International LLC, 2009. .

[17] J. Deng, M. M. . Lee, and S. S. . Moy, "Stress analysis of steel beams reinforced with a bonded CFRP plate," Compos. Struct., vol. 65, no. 2, pp. 205–215, Aug. 2004.

[18] ABAQUS, Theory Manual, User Manual and Example Manual, Version 6. Dassault Systemes Simulia Corp, 2013.

[19] BS EN 1090-2, "Execution of steel structures and aluminium structures: Technical requirements for steel structures," British Standards Institution, London, UK, 2008.